# Mass–spring–damper modelling of the human body to study running and hopping – an overview

**A A Nikooyan**‡ and **A A Zadpoor***‡
Department of Biomechanical Engineering, Delft University of Technology (TU Delft), Delft, The Netherlands

*The manuscript was received on 28 April 2011 and was accepted after revision for publication on 1 September 2011.*

DOI: 10.1177/0954411911424210

**Abstract:** Several mass–spring–damper models have been developed to study the response of the human body to the collision with the ground during hopping, trotting, or running. The mass, spring, and damper elements represent the masses, stiffness properties, and damping properties of hard and soft tissues. The masses that models are composed of are connected to each other via springs and dampers. The present paper reviews the various types of mass–spring–damper models including one-body and multi-body models. The models are further categorized as being either passive or active. In passive models, the mechanical properties (stiffness and damping) of soft tissues remain constant regardless of the type of footwear, ground stiffness, etc. In active models, the mechanical properties adapt to external loads. The governing equations of motion of all models as well as their parameters are presented. The specific ways that the models take account of the shoe–ground interactions are discussed as well. The methods used for determination of different modelling parameters are briefly surveyed. The advantages and disadvantages of the different types of mass–spring–damper models are also discussed. The paper concludes with a brief discussion of possible future research trends in the area of mass–spring–damper modelling.

**Keywords:** mechanical modelling, stiffness, damping, passive and active models, shoe–ground model, ground reaction force

## 1 INTRODUCTION

Locomotion is one of the most important functions of the musculoskeletal system and has been extensively studied using both experimental and modelling techniques. Locomotion is studied primarily to understand either the physiological mechanism of locomotion or the locomotive deficiencies of the musculoskeletal system. Despite this extensive effort in understanding the locomotion mechanism, it is not yet well understood even in physiological conditions. This is partly due to the complexity of the musculoskeletal system and partly due to the interplay between the musculoskeletal and neural systems.

The experimental techniques used to study locomotion include the force plate measurement of ground reaction forces, human motion tracking systems, and electromyography. Although experimental techniques are valuable in understanding many aspects of locomotion, they have some limitations. First, not every quantity can be easily measured. For example, there is no non-invasive easy way of measuring muscle forces *in vivo*. Second, experiments cannot be used to study the isolated effect of parameters. For example, it is hardly possible to study experimentally the independent effects of body mass distribution on locomotion [**1**], because one cannot change body mass distribution while keeping the other parameters constant. It is much easier to run parametric studies using a model. Third,

**Corresponding author: Department of Biomechanical Engineering, Delft University of Technology (TU Delft), Mekelweg 2, 2628 CD Delft, The Netherlands.*
*email: a.a.zadpoor@tudelft.nl*
‡*Both authors have equally contributed to this manuscript and should therefore be considered as joint first authors.*

experiments may need access to a large number of participants and to specific experimenting conditions. For example, experimental study of the effects of microgravity on the musculoskeletal system requires prolonged access to microgravity that is extremely difficult to secure. In modelling, one can simulate microgravity by changing the gravitation acceleration, $\boldsymbol{g}$.

One of the approaches used for modelling of the musculoskeletal system during locomotion is the so-called mass–spring–damper (MSD) modelling approach. In this approach, a limited number of masses represent the inertia properties of the different segments of the human body including hard tissues and soft tissues. Springs and dampers represent the mechanical properties of the different segments including bones, muscles, tendons, and ligaments. Such relatively simple models of the human body are very useful in studying the general principles of locomotion [**2**]. In particular, they can be used to determine which features of a moving human have significant impact on some particular aspects of her/his locomotion [**2**]. Therefore, MSD models have been used extensively for describing different aspects of locomotion including the dynamics of running and hopping and the loading of the human body during these activities. Despite their widespread use, no overview of the MSD models of the human body is currently available in the literature.

Walking, posture, and running and hopping have their own requirements that are often quite remote from each other. The biomechanical models that are developed for describing these phenomena are therefore quite different. The present paper is concerned only with running and hopping. Moreover, the main focus is on the MSD models themselves and not as much on the results that are obtained using these models. The reviewed models include one-body and multi-body models and passive as well as active models. The modelling assumptions, governing equations of motion, and model parameters are presented. The advantages and disadvantages of the different classes of MSD models are discussed as well. The paper ends with a brief section on future research trends in MSD modelling of running and hopping.

## 2 PASSIVE MODELS

As implied by their name, passive MSD models of the human body do not include the effects of any active element such as muscle. The response of the model is entirely dependent on the passive representation of the body segments and is therefore the same regardless of environmental parameters such as the stiffness of the ground or the type of footwear. Many MSD models that have been developed so far belong to this category. Based on the number of their masses, passive models can be categorized as either one-body or multi-body models. Each of the two following subsections covers one of these two categories of passive models.

### 2.1 One-body models

Perhaps the simplest model of the interaction between the human body and the ground during bouncing gait (hopping, trotting, and running) is built by attaching a lumped mass representing the body mass to an in-plane weightless spring representing the body stiffness. This type of model was originally proposed by Blickhan [**3**] and McMahon and Cheng [**4**]. Two common types of one-body mass–spring models have been developed:

(a) one-dimensional (1D) motion model (Fig. 1(a)) used for in-place hopping when there is no forward motion;
(b) two-dimensional (2D) motion model (Fig. 1(b)) used to study in-plane forward running.

The governing equations of the motion of these two types of one-body mass–spring models are presented in section 2.1.1.

One-body models are probably the most widely used MSD models. They are used for different purposes, but the most widespread application of the one-body mass–spring models is perhaps in determination of the lower-extremity stiffness and prediction of the ground reaction force (GRF) during hopping and running. In addition, one-body models are used to study the stride frequency in running [**5**], the energy cost of running [**6**], the aerobic demand of running [**7**], and the effects of hopping [**8**] and running [**9**] speed, various surfaces [**10**, **11**], and fatigue [**12**] on the dynamics of the human

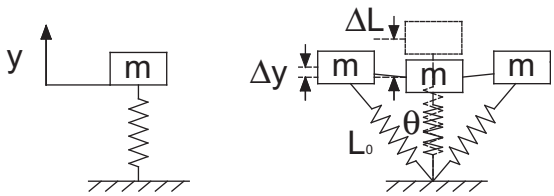


**Fig. 1** Schematic representation of the (a) 1D motion and (b) 2D motion passive one-body mass–spring models [**3**, **4**]

body. Running in reduced-gravity conditions [**13**, **14**] and the stability of running [**15**] are also studied.

Given the importance of one-body models for determination of the body stiffness, this application of the one-body models is emphasized in the present review. Farley and colleagues [**16**] used the 1D motion model (hopping model) for prediction of the vertical stiffness and force of the human body in in-place hopping. In a more recent study [**17**], the 2D motion model was recruited to calculate the vertical and leg stiffness during running. The vertical stiffness is defined as the ratio of the vertical leg spring compression to peak vertical GRF at the middle of the stance phase [**3**, **17**, **18**]. Butler *et al.* [**18**] surveyed the available methods for calculating the vertical and leg stiffness using the one-body mass–spring models. These methods are summarized in section 2.1.2 of the present paper. In a later study [**19**], five different methods for calculation of the leg stiffness were compared with each other based on the running pattern estimated by the one-body mass–spring model. Using experimental data, Hunter [**20**] modified a forward (2D motion) running model for more accurate prediction of the vertical stiffness and GRF in distance running.

Given the simplicity of one-body mass–spring models, it is natural to question their accuracy in predicting the characteristics of running. An extensive work for quantitative evaluation of the one-body mass–spring models was carried out by Bullimore and Burn [**2**, **21**]. By comparing the model predictions with the experimental data in normal and simulated reduced gravity [**13**], Bullimore and Burn [**2**] concluded that one-body models predict the parameters of the running human (e.g. vertical active peak GRF, stance time, contact length, etc.) reasonably well in the normal as well as simulated reduced-gravity conditions. However, they showed that one-body mass–spring models (systematically) overestimate the peak horizontal GRF, the peak vertical displacement of the centre of mass during stance phase, and the aerial time.

### 2.1.1 Equations of motion

(a) *1D motion model (hopping model)*. The equation of motion for a 1D motion model (Fig. 1(a)) can be written as follows

$$m\ddot{y} + k_{\text{ver}}y = m\boldsymbol{g} \tag{1}$$

where $k_{\text{ver}}$ is the vertical stiffness and is calculated as

$$k_{\text{leg}} = \frac{F_{\max}}{\Delta y_{\max}} \tag{2}$$

where $F_{\max}$ is the maximum vertical force and $\Delta y_{\max}$ is the maximum spring deformation.

(b) *2D motion model (running model)*. For the 2D motion model, the equation of motion may be written as follows

$$m\ddot{y} + k_{\text{leg}}y = m\boldsymbol{g} \tag{3}$$

where $k_{\text{leg}}$ is the leg stiffness and is calculated as

$$k_{\text{leg}} = \frac{F_{\max}}{\Delta L} \tag{4}$$

where $F_{\max}$ is the maximum vertical force and $\Delta L$ is the vertical displacement of the mass that is formulated as

$$\Delta L = \Delta y + L_0(1 - \cos\theta) \tag{5}$$

where $L_0$ is the standing leg length and the angle $\theta$ is calculated as follows

$$\theta = \sin^{-1}\left(\frac{\dot{x}t_{\text{c}}}{2L_0}\right) \tag{6}$$

where $\dot{x}$ is the forward speed and $t_{\text{c}}$ is the contact time with the ground.

### 2.1.2 Calculation of vertical and leg stiffness

Butler *et al.* [**18**] surveyed the different methods that had been used to approximate the vertical stiffness $k_{\text{ver}}$ of 1D motion one-body mass–spring models. They identified three general methods in the literature that are briefly discussed here.

The first and simplest method is proposed by McMahon and Cheng [**4**] and was presented in section 2.1.1 (equation (2)). As proposed by Cavagna [**22**], the vertical displacement can be calculated by integrating the vertical acceleration data.

The second method developed by Cavagna *et al.* [**23**] uses the subject's mass $m$ and the period of the vertical vibration $T$ to calculate the vertical stiffness and is formulated as follows

$$k_{\text{ver}} = m\left(\frac{2\pi}{T}\right)^2 \tag{7}$$

In this method, the vertical GRF is assumed to be a sine wave with its peak happening at the midpoint of the stance phase.

The third method, which was presented by McMahon *et al.* [**24**], calculates the vertical stiffness

by using the subject's mass and the natural frequency of vibrations $\omega_0$ as follows

$$k_{ver} = m\omega_0^2 \tag{8}$$

where natural frequency $\omega_0$ is the inverse of step duration (time interval between two successive strikes).

The leg stiffness $k_{leg}$ in 2D motion one-body models is calculated using the method developed by McMahon and Cheng [**4**] presented in section 2.1.1 (equations (3) to (6)).

### 2.2 Multi-body models

The human body is a very complex system with many masses (bodies). Therefore, an oversimplified model, like a simple one-body mass–spring model, cannot fully explain the various aspects of such a complex system. For example, the vertical GRF versus time typically includes two force peaks. Different names have been used for these two peaks [**25**]: the first and second peaks [**1**, **26**], impact and active force peaks [**27**–**30**], passive and active peaks [**31**], and impact and propulsion peaks [**32**, **33**], respectively. It is shown that while the active GRF peaks predicted by simple one-body mass–spring models during the stance phase of running are comparable to those obtained from experiments [**2**], one-body models are not capable of accurately predicting the impact (passive) GRF peaks (Fig. 2) [**34**]. This seems to be related to the simple sinusoidal shape of the GRF curves produced by this kind of model.

Several multi-body mass–spring–damper models (Tables 1 to 3, Figs 3 to 7) have therefore been proposed for more detailed description of the phenomena observed during human locomotion.

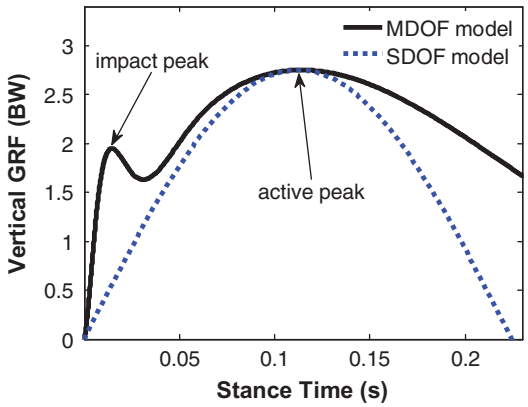


**Fig. 2** Typical vertical GRF versus stance time for one-body (SDOF) and multi-body models (MDOF). The four-body model by Zadpoor *et al.* [**26**] was used to generate the plot for the multi-body case

The simplest examples of multi-body models are two-body models (Fig. 3). Mizrahi and Susak [**35**] developed a two-body model (Fig. 3(a)) for estimation of the peak accelerations during impact. A similar model (Fig. 3(b)) was used for prediction of the GRF during jumping on hard surfaces [**36**]. The model was made of two masses, $m_1$ and $m_2$, representing the upper and lower body, respectively. The masses were connected to each other and to the ground via linear springs, $k_2$ and $k_1$, and dampers, $c_2$ and $c_1$. A simpler but similar model (Fig. 3(c)) was introduced by Derrick *et al.* [**37**] in which the masses were connected only via a linear spring, $k_2$. $c_1$ and $k_1$ are the connection between mass $m_1$ and the ground. That model was used to study the GRF during running with different stride lengths.

A three-body model was developed by Kim *et al.* [**38**] (Fig. 4(a)) to investigate the shock absorption of the human body as well as the effects of stiffness and damping coefficients of the ground–shoe complex on loading. Of the three masses that are present in the model (Fig. 4(a)), two masses $m_1$ and $m_2$ represent the foot and tibia, and the other mass $m_3$ represents the rest of the body. The masses are connected together via linear springs and dampers. The shoe–ground interaction is modelled using a spring and a damper, $k_1$ and $c_1$.

The four-body model developed by Liu and Nigg (LN model) [**1**, **39**] (Fig. 5(a)) is probably the most widely used multi-body MSD model of the human body during hopping and running. The model consists of four masses, five springs, and four dampers. Two important novelties separate this model from the previously discussed models: first, the upper- and lower-body masses have been divided into rigid ($m_1$ and $m_3$) and wobbling ($m_2$ and $m_4$) masses. The wobbling masses represent all non-rigid parts of the body such as muscles, skin, blood vessels, etc. Second, the shoe–ground interaction is modelled with a non-linear function (Table 3) that relates the GRF, $F_g$, to the touch-down velocity, $\dot{x}_1$, and shoe hardness parameters, *a*, *b*, *c*, *d*, and *e*. Liu and Nigg used this model to study the effects of the stiffness and damping coefficients [**39**] as well as the effects of mass and mass distributions [**1**] on the GRF during running and hopping. This model is used as the basis of a variety of further studies.

Yue and Mester [**40**] presented two modified versions of the LN model (Figs 4(b) and 5(b)). The first model is a four-body model in which the shoe–ground element is replaced by a vibrating platform that is fixed to the lower-body rigid mass (Fig. 5(b)). The second model is a three-body model in which the upper body is represented by a single rigid mass

**Table 1** The mass **M**, stiffness **K**, and damping **C** parameters of the models discussed in the paper presented in matrix format. The weight column vectors ***W*** of multi-body models (Figs 3 to 7) are also presented

| Reference | **M** | **C** | **K** | ***W*** |
|---|---|---|---|---|
| [**35**] (Fig. 3(a)) | $\begin{bmatrix} m_1 & 0 \\ 0 & m_2 \end{bmatrix}$ | $\begin{bmatrix} c_1+c_2 & -c_2 \\ -c_2 & c_2 \end{bmatrix}$ | $\begin{bmatrix} k_1+k_2 & -k_2 \\ -k_2 & k_2 \end{bmatrix}$ | $\begin{bmatrix} 0 \\ 0 \end{bmatrix}$ |
| [**36**] (Fig. 3(b)) | $\begin{bmatrix} m_1 & 0 \\ 0 & m_2 \end{bmatrix}$ | $\begin{bmatrix} c_1+c_2 & -c_2 \\ -c_2 & c_2 \end{bmatrix}$ | $\begin{bmatrix} k_1+k_2 & -k_2 \\ -k_2 & k_2 \end{bmatrix}$ | $\begin{bmatrix} m_1 g \\ m_2 g \end{bmatrix}$ |
| [**37**] (Fig. 3(c)) | $\begin{bmatrix} m_1 & 0 \\ 0 & m_2 \end{bmatrix}$ | $\begin{bmatrix} c_1 & 0 \\ 0 & 0 \end{bmatrix}$ | $\begin{bmatrix} k_1+k_2 & -k_2 \\ -k_2 & k_2 \end{bmatrix}$ | $\begin{bmatrix} m_1 g \\ m_2 g \end{bmatrix}$ |
| [**38**] (Fig. 4(a)) | $\begin{bmatrix} m_1 & 0 & 0 \\ 0 & m_2 & 0 \\ 0 & 0 & m_3 \end{bmatrix}$ | $\begin{bmatrix} c_1+c_2 & -c_2 & 0 \\ -c_2 & c_2+c_3 & -c_3 \\ 0 & -c_3 & c_3 \end{bmatrix}$ | $\begin{bmatrix} k_1+k_2 & -k_2 & 0 \\ -k_2 & k_2+k_3 & -k_3 \\ 0 & -k_3 & k_3 \end{bmatrix}$ | $\begin{bmatrix} m_1 g \\ m_2 g \\ m_3 g \end{bmatrix}$ |
| [**40**] (Fig. 4(b)) | $\begin{bmatrix} m_1 & 0 & 0 \\ 0 & m_2 & 0 \\ 0 & 0 & m_3+m_4 \end{bmatrix}$ | $\begin{bmatrix} c_1+c_2 & -c_2 & -c_1 \\ -c_2 & c_2 & 0 \\ -c_1 & 0 & c_1 \end{bmatrix}$ | $\begin{bmatrix} k_1+k_2 & -k_2 & -k_1 \\ -k_2 & k_2+k_3 & -k_3 \\ -k_1 & -k_3 & k_1+k_3 \end{bmatrix}$ | $\begin{bmatrix} m_1 g \\ m_2 g \\ (m_3+m_4) g \end{bmatrix}$ |
| [**39**] (Fig. 5(a)) | $\begin{bmatrix} m_1 & 0 & 0 & 0 \\ 0 & m_2 & 0 & 0 \\ 0 & 0 & m_3 & 0 \\ 0 & 0 & 0 & m_4 \end{bmatrix}$ | $\begin{bmatrix} c_1+c_2 & -c_2 & -c_1 & 0 \\ -c_2 & c_2 & 0 & 0 \\ -c_1 & 0 & c_1+c_4 & -c_4 \\ 0 & 0 & -c_4 & c_4 \end{bmatrix}$ | $\begin{bmatrix} k_1+k_2 & -k_2 & -k_1 & 0 \\ -k_2 & k_2+k_3 & -k_3 & 0 \\ -k_1 & -k_3 & k_1+k_3+k_4+k_5 & -(k_4+k_5) \\ 0 & 0 & -(k_4+k_5) & k_4+k_5 \end{bmatrix}$ | $\begin{bmatrix} m_1 g - F_g \\ m_2 g \\ m_3 g \\ m_4 g \end{bmatrix}$ |
| [**40**] (Fig. 5(b)) | $\begin{bmatrix} m_1 & 0 & 0 & 0 \\ 0 & m_2 & 0 & 0 \\ 0 & 0 & m_3 & 0 \\ 0 & 0 & 0 & m_4 \end{bmatrix}$ | $\begin{bmatrix} c_1+c_2 & -c_2 & -c_1 & 0 \\ -c_2 & c_2 & 0 & 0 \\ -c_1 & 0 & c_1+c_4 & -c_4 \\ 0 & 0 & -c_4 & c_4 \end{bmatrix}$ | $\begin{bmatrix} k_1+k_2 & -k_2 & -k_1 & 0 \\ -k_2 & k_2+k_3 & -k_3 & 0 \\ -k_1 & -k_3 & k_1+k_3+k_4+k_5 & -(k_4+k_5) \\ 0 & 0 & -(k_4+k_5) & k_4+k_5 \end{bmatrix}$ | $\begin{bmatrix} m_1 g \\ m_2 g \\ m_3 g \\ m_4 g \end{bmatrix}$ |
| [**43**] (Fig. 6) | $\begin{bmatrix} m_1 & 0 & 0 & 0 & 0 \\ 0 & m_2 & 0 & 0 & 0 \\ 0 & 0 & m_3 & 0 & 0 \\ 0 & 0 & 0 & m_4 & 0 \\ 0 & 0 & 0 & 0 & m_5 \end{bmatrix}$ | $\begin{bmatrix} c_1+c_2 & -c_2 & -c_1 & 0 & 0 \\ -c_2 & c_2 & 0 & 0 & 0 \\ -c_1 & 0 & c_1+c_4 & -c_4 & 0 \\ 0 & 0 & -c_4 & c_4 & 0 \\ 0 & 0 & 0 & 0 & 0 \end{bmatrix}$ | $\begin{bmatrix} k_1+k_2 & -k_2 & -k_1 & 0 & 0 \\ -k_2 & k_2+k_3 & -k_3 & 0 & 0 \\ -k_1 & 0 & -k_3 & k_1+k_3+k_4+k_5 & -(k_4+k_5) \\ 0 & 0 & -(k_4+k_5) & k_4+k_5 & 0 \\ 0 & 0 & 0 & 0 & 0 \end{bmatrix}$ | $\begin{bmatrix} m_1 g + F_s \\ m_2 g \\ m_3 g \\ m_4 g \\ m_5 g - F_s + F_g \end{bmatrix}$ |
| [**44**] (Fig. 7) | $\begin{bmatrix} m_1 & 0 & 0 & 0 & 0 \\ 0 & m_2 & 0 & 0 & 0 \\ 0 & 0 & m_3 & 0 & 0 \\ 0 & 0 & 0 & m_4 & 0 \\ 0 & 0 & 0 & 0 & m_5 \end{bmatrix}$ | $\begin{bmatrix} c_2 & -c_2 & 0 & 0 & 0 \\ -c_2 & c_2+c_3 & -c_3 & 0 & 0 \\ 0 & -c_3 & c_3+c_4 & -c_4 & 0 \\ 0 & 0 & -c_4 & c_4+c_5 & -c_5 \\ 0 & 0 & 0 & -c_5 & c_5 \end{bmatrix}$ | $\begin{bmatrix} k_2 & -k_2 & 0 & 0 & 0 \\ -k_2 & k_2+k_3 & -k_3 & 0 & 0 \\ 0 & -k_3 & k_3+k_4 & -k_4 & 0 \\ 0 & 0 & -k_4 & k_4+k_5 & -k_5 \\ 0 & 0 & 0 & -k_5 & k_5 \end{bmatrix}$ | $\begin{bmatrix} m_1 g - F_g \\ m_2 g \\ m_3 g \\ m_4 g \\ m_5 g \end{bmatrix}$ |

**Table 2** The entries of the mass, stiffness, and damping matrices introduced in Table 1 for various multi-body MSD models ($m$, mass; $k$, stiffness coefficient; $c$, damping coefficient; NA, not available)

| Reference | Description | $m_i$ (kg) | $c_i$ (kNs/m) | $k_i$ (kN/m) |
|---|---|---|---|---|
| [**35**] (Fig. 3(a)) | Subject A: | $m_1 \approx 62$<br>$m_2 \approx 10$ | $c_1 \approx 0.81$<br>$c_2 \approx 0.94$ | $k_1 \approx 8.45$<br>$k_2 \approx 45.2$ |
| | Subject B: | $m_1 \approx 56$<br>$m_2 \approx 9$ | $c_1 \approx 0.79$<br>$c_2 \approx 0.78$ | $k_1 \approx 5.32$<br>$k_2 \approx 42.3$ |
| [**36**] (Fig. 3(b)) | There were insufficient data in the original paper to calculate the magnitude of $c_1$ | $m_1 = 12.05$<br>$m_2 = 63.45$ | $c_1 =$ NA<br>$c_2 = 0.84$ | $k_1 = 122.00$<br>$k_2 = 11.22$ |
| [**37**] (Fig. 3(c)) | Values are given for the average masses (ten subjects) and for the preferred stride length condition | $m_1 = 15$<br>$m_2 = 61$ | $c_1 = 0.76$ | $k_1 = 78.4$<br>$k_2 = 34.1$ |
| [**38**] (Fig. 4(a)) | | $m_1 = 1.12$<br>$m_2 = 3.26$<br>$m_3 = 50.62$ | $c_1 = 0.17$<br>$c_2 = 0.44$<br>$c_3 = 0.04$ | $k_1 = 0.05$<br>$k_2 = 94.10$<br>$k_3 = 40.10$ |
| [**39**], [**40**] (Figs 4(b), 5(a), and 5(b)) | | $m_1 = 6.15$<br>$m_2 = 6.00$<br>$m_3 = 12.58$<br>$m_4 = 50.34$ | $c_1 = 0.30$<br>$c_2 = 0.65$<br>$c_4 = 1.90$ | $k_1 = 6$<br>$k_2 = 6$<br>$k_3 = 10$<br>$k_4 = 10$<br>$k_5 = 18$ |
| [**43**] (Fig. 6) | | $m_1 = 6.15$<br>$m_2 = 6.00$<br>$m_3 = 12.58$<br>$m_4 = 50.34$<br>$m_5 = 0.30$ | $c_1 = 0.30$<br>$c_2 = 0.65$<br>$c_4 = 1.90$ | $k_1 = 6$<br>$k_2 = 6$<br>$k_3 = 10$<br>$k_4 = 10$<br>$k_5 = 18$ |
| [**44**] (Fig. 7) | | $m_1 = 1.8$<br>$m_2 = 6.3$<br>$m_3 = 5.4$<br>$m_4 = 22.5$<br>$m_5 = 54$ | $c_2 = 10.0$<br>$c_3 = 0.5$<br>$c_4 = 1.5$<br>$c_5 = 1.1$ | $k_2 = 1.0 \times 10^5$<br>$k_3 = 50$<br>$k_4 = 75$<br>$k_5 = 10$ |

connected to the lower-body wobbling and rigid masses (Fig. 4(b)). They used these modified versions of the LN model to study the effects of taking account of the wobbling masses in the vibration analysis of the human body. The outcome of that study showed that implementing the wobbling mass in the upper body considerably reduces the loads sustained by the upper-body rigid mass. In a later study, Yue and Mester [**41**] used the modified four-body model (Fig. 5(b)) to run a modal analysis of the human body vibrations. Even though these models are not directly used to study running or hopping, they are still mentioned in this review because of their importance in the development of some other multi-body MSD models. These models specifically showed the importance of the inclusion of the wobbling mass in multi-body MSD models.

Zadpoor and Nikooyan [**42**] showed that the LN model was not correctly simulated and that if it is correctly simulated, it will not match experimental results. In a following study, Zadpoor *et al.* [**26**] modified the parameters of the LN model such that the predictions of the model agreed with experimental observations.

In a recent study, Ly *et al.* [**43**] developed a five-body model of the human body (Fig. 6) based on the LN model in which the ground reaction model in the LN model is replaced with a two-body MSD system representing the stiffness of the shoe midsole, $k_6$, $b_6$, and $c_6$ (Table 3), and that of the ground, $k_s$ (Table 3). In this model, the force between the foot and the shoe midsole is modelled using a non-linear function (Table 3). The ground–shoe interaction is represented using a simple linear function of the ground stiffness (Table 3). The aim of such modification is to investigate the independent effects of the shoe midsole and the ground stiffness on the impact force during running. The effects of six different soil types representing different ground stiffness values as well as the effects of four different shoe types on the GRF were studied.

The last example of the multi-body MSD models that are discussed here is the five-body model developed by Klute and Berge [**44**]. The model (Fig. 7) is composed of upper- and lower-body rigid ($m_4$ and $m_3$) and wobbling ($m_5$ and $m_2$) masses, the mass $m_1$ of the prosthetic foot, the connecting spring and dampers, and the prosthetic foot–ground interaction element. The vertical GRF, $F_g$, acting on the prosthetic shoe and foot is represented by a non-linear function of the prosthetic foot and shoe parameters (Table 3). The model is developed to study the

**Table 3** The formulation and parameters of the shoe–ground and shoe–foot reaction models used in some of the multi-body models (Figs 4 to 7)

| Reference | Formulation | Parameters |
|---|---|---|
| [**39**], [**40**] (Figs 4(b), 5(a), and 5(b)) | The vertical GRF (acting on the shoe and foot): $F_g = \begin{cases} A_c\left(ax_1^b + cx_1^d\dot{x}_1^e\right), & x_1 > 0 \\ 0, & x_1 \leqslant 0 \end{cases}$ | $A_c = 2.00$<br>$a = 1.00\times10^6$<br>$b = \begin{cases} 1.56, & \text{soft shoe} \\ 1.38, & \text{hard shoe} \end{cases}$<br>$c = 2.00\times10^4$<br>$d = \begin{cases} 0.73, & \text{soft shoe} \\ 0.75, & \text{hard shoe} \end{cases}$<br>$e = 1.00$ |
| [**43**] (Fig. 6) | The vertical GRF:<br>$F_g = -k_s x_5$<br>The values of the parameter are given for six different soil types<br><br>The force between the foot and the shoe sole:<br>$F_s = -k_6(x_1 - x_5)\left(\frac{x_1 - x_5}{R_0}\right)^{b_6 - 1} - c_6(\dot{x}_1 - \dot{x}_5)$<br>The values of the parameter are given for four different shoe types | $k_s = \begin{Bmatrix} 99 \\ 143 \\ 210 \\ 359 \\ 429 \\ 880 \end{Bmatrix}$, $k_6 = \begin{Bmatrix} 222 \\ 218 \\ 362 \\ 403 \end{Bmatrix}$<br>$b_6 = \begin{Bmatrix} 2.1679 \\ 1.9519 \\ 2.3018 \\ 2.4346 \end{Bmatrix}$, $c_6 = \begin{Bmatrix} 914 \\ 1370 \\ 1870 \\ 2170 \end{Bmatrix}$<br>$R_0 = 40$ mm |
| [**44**] (Fig. 7) | The vertical GRF (acting on the prosthetic shoe and foot):<br>$F_g = ax_1^b + \text{sgn}(\dot{x}_1)cx_1^d\lvert\dot{x}_1\rvert^e$<br>The values of the parameter are given for seven different prosthetic feet and three different shoes | $a = \begin{Bmatrix} 23.5\times10^5 \\ 8.4\times10^5 \\ 5.2\times10^5 \\ 7.1\times10^5 \\ 53.8\times10^5 \\ 7.9\times10^5 \\ 4.0\times10^5 \\ 0.16\times10^5 \\ 0.50\times10^5 \\ 0.85\times10^5 \end{Bmatrix}$, $b = \begin{Bmatrix} 1.72 \\ 1.59 \\ 1.53 \\ 1.59 \\ 2.05 \\ 1.70 \\ 1.68 \\ 0.90 \\ 1.06 \\ 1.15 \end{Bmatrix}$, $c = \begin{Bmatrix} 2.0\times10^4 \\ 2.0\times10^4 \\ 54.9\times10^4 \\ 3.6\times10^4 \\ 1.1\times10^4 \\ 5.0\times10^4 \\ 0.05\times10^4 \\ 3.8\times10^4 \\ 9.9\times10^4 \\ 12.3\times10^4 \end{Bmatrix}$<br>$d = \begin{Bmatrix} 0.91 \\ 0.95 \\ 1.56 \\ 1.05 \\ 0.90 \\ 1.14 \\ 0.44 \\ 1.25 \\ 1.71 \\ 1.81 \end{Bmatrix}$, $e = \begin{Bmatrix} 1.00 \\ 1.00 \\ 1.00 \\ 1.00 \\ 1.00 \\ 1.00 \\ 1.00 \\ 0.73 \\ 0.65 \\ 0.61 \end{Bmatrix}$ |

effects of the prosthetic feet or shoes on the impact force during amputee locomotion. The parameters of seven different prosthetic feet and three different shoe types are used (Table 3).

### 2.2.1 *Governing equations of motion*

For a multi-body system, the governing equations of motion may be written in a general form as follows

$$\mathbf{M}\ddot{\boldsymbol{X}} + \mathbf{C}\dot{\boldsymbol{X}} + \mathbf{K}\boldsymbol{X} = \boldsymbol{W} \tag{9}$$

where **M** is the mass matrix, **C** is the matrix of damping coefficients, **K** is the stiffness matrix, $\boldsymbol{X}$, $\dot{\boldsymbol{X}}$, and $\ddot{\boldsymbol{X}}$ are respectively the displacement, velocity, and acceleration vectors. $\boldsymbol{W}$ is a column vector that contains the weight of the masses included in the model. Each element of $\boldsymbol{W}$ is not a scalar component of a spatial vector along the axes of a Cartesian coordinate system but only the magnitude of the weight of (one of) the masses. In some cases (Table 1), the force produced by the element of the model that represents ground–shoe interactions is also included in $\boldsymbol{W}$.

For the various models shown in Figs 3 to 7, the mass, damping, and stiffness matrices as well as the weight vectors are listed in Table 1. Even though the left side of equation (9) is linear, the overall equation is often non-linear due to the dependence of the force on the position and velocity of certain masses within the model. Having the initial conditions such as touchdown velocities of the masses, the governing equations of the motion can be solved numerically using non-linear

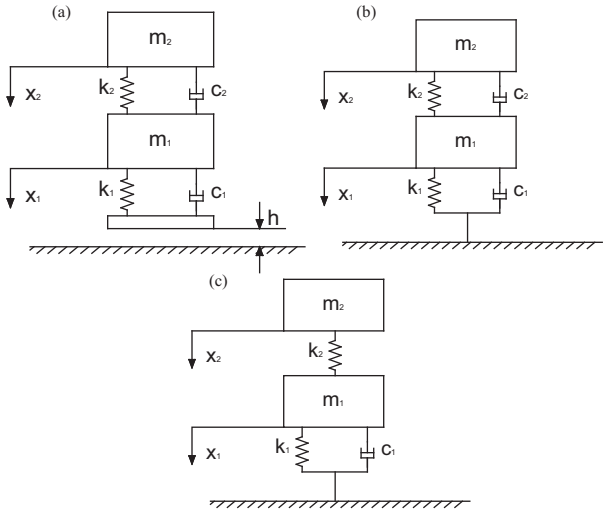


**Fig. 3** Schematic representation of the passive two-body MSD models developed by (a) Mizrahi and Susak [**35**], (b) Nevzat Özgüven and Berme [**36**], and (c) Derrick *et al.* [**37**]

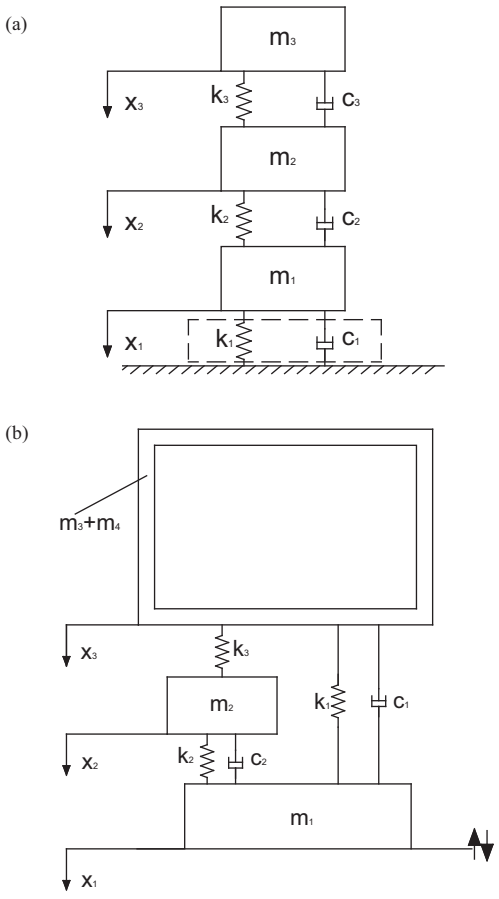


**Fig. 4** Schematic representation of the passive three-body MSD model developed by (a) Kim *et al.* [**38**] and (b) Yue and Mester [**40**]

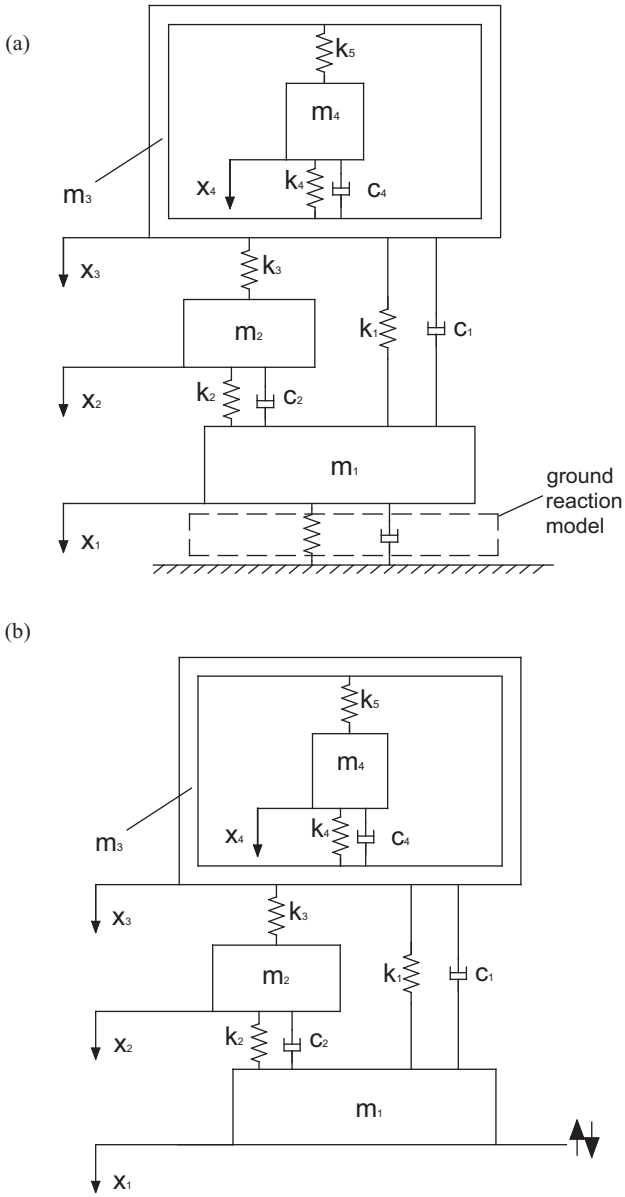


**Fig. 5** Schematic representation of the passive four-body MSD model developed by (a) Liu and Nigg [**1**, **39**] and (b) Yue and Mester [**40**]

ordinary differential equation solvers such as Runge–Kutta solvers.

### 2.2.2 *Determination of the modelling parameters*

The values of the modelling parameters for each multi-body model (Table 1) are summarized in Table 2. In this section, the methods used for determination of these parameters are briefly discussed.

In the two-body model developed by Mizrahi and Susak [**35**] (Fig. 3(a)), a 1:6 ratio between the lower and upper masses $m_1$ and $m_2$ (Table 2) was assumed. Having the magnitude of the whole-body

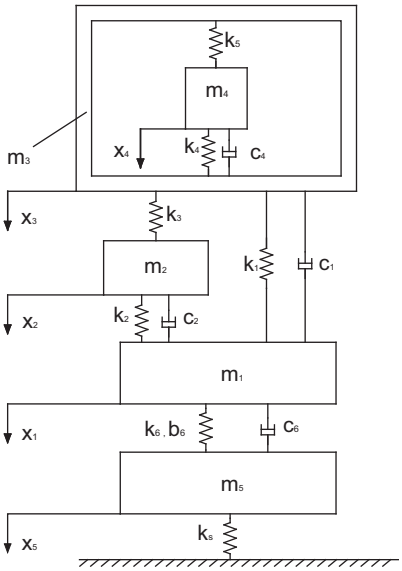


**Fig. 6** Schematic representation of the passive five-body MSD model developed by Ly *et al.* [**43**]

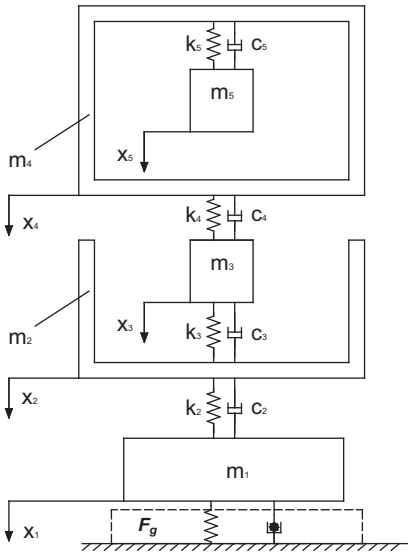


**Fig. 7** Schematic representation of the passive five-body MSD model developed by Klute and Berge [**44**]

mass of two measured subjects (subjects A and B, Table 2) and the mass ratio, the $m_1$ and $m_2$ values were determined (Table 2). For each subject, the stiffness and damping coefficients (Table 2) were estimated by minimizing the difference between the peaks of the model-predicted and measured accelerations.

The values of the lower- and upper-body masses $m_1$ and $m_2$ (Table 2) in the two-body model by Nevzat Özgüven and Berme [**36**] (Fig. 3(b)) were calculated by using the average masses of four measured subjects (75.5 kg). A mass ratio of 0.19 between $m_1$ and $m_2$ was estimated from a set of experimental data. The values of the spring coefficients $k_1$ and $k_2$ are the mean of the stiffness values identified in the original paper for different subjects and different combinations of natural frequencies $\omega_1$ and $\omega_2$ [**36**]. The damping coefficients, $c$, were calculated as follows

$$c = \frac{2\zeta k}{\omega} \tag{10}$$

where $\zeta$ is the damping ratio. A damping ratio of 0.5 was used for the second mode, because it resulted in the best correspondence between the predictions and experimental results. Given these data, one can calculate the damping coefficient of the upper body, $c_2$. The mean value or the damping coefficient $c_2$ is given in Table 2. However, the damping ratio of the first mode was not given in the original paper. Therefore, the damping coefficient of the lower body, $c_1$, could not be calculated.

In the two-body model by Derrick *et al.* [**37**] (Fig. 3(c)), the optimization results showed that the best agreement between the simulated and measured vertical GRF is obtained when the lower-body mass $m_1$ is 20 per cent of the total body mass. Ten subjects participated in the measurements of that study. Considering an average body mass of 76 kg, the lower- and upper-body masses were estimated (Table 2). The best fit between the model predictions and the GRF measurements was used to determine the stiffness and damping parameters at different stride lengths. The values of $k_1$, $k_2$, and $c_1$ presented in Table 2 relate to the preferred stride length.

The distribution of the masses $m_1$, $m_2$, and $m_3$ (Table 2) in the three-body model by Kim *et al.* [**38**] (Fig. 4(a)) was adopted from the anthropometric data in reference [**45**]. The total-body mass was considered to be about 55 kg. The values of the stiffness and damping parameters were identified using the data measured during three consecutive heel strikes. The mean values of the stiffness and damping parameters $k_1$, $k_2$, $k_3$, $c_1$, $c_2$, and $c_3$ are listed in Table 2.

In the LN model [**1**, **39**], the total body was assumed to be 75 kg. The values of the masses were adopted from a study by Cole [**46**] in which the distribution of the wobbling and rigid masses was estimated based on the formulas developed in references [**47**] and [**48**]. The muscle–tendon properties presented by Cole [**46**] were used to approximate the stiffness values of the springs connecting the upper-body wobbling and rigid masses, i.e. $k_4$ and $k_5$. The damping coefficient $c_4$ was estimated using the critical damping assumption [**49**]. The spring constant $k_1$ and damping coefficient $c_1$ were

similar to the values used for the overall stiffness and damping properties of the human leg in references [**4**] and [**5**]. The parameters of the hard and soft shoe models, i.e. *a*, *b*, *c*, *d*, and *e* (Table 3), were determined using a least-square algorithm that fitted the simulated force–deformation curves of pendulum impact tests to the data presented in reference [**50**].

The same values of model parameters as in the LN model were used in the three- and four-body models developed by Yue and Mester [**40**] (Figs 4(b) and 5(b)).

In the five-body model developed by Ly *et al.* [**43**] (Fig. 6), the same values as in the LN model were used for $m_1$ to $m_4$, $k_1$ to $k_5$, $c_1$, $c_2$, and $c_4$ (Table 2). The ground stiffness $k_s$ (Table 3) was estimated for six different soil types through a finite element method and by using the elastic moduli of the different types of soil obtained from the literature. Four running shoes with the same shapes and masses were tested to determine the viscoelastic properties of the shoe midsole, $k_6$ and $b_6$. The tests were performed using a hydraulic machine and by applying a sinusoidal force to the rear part of the sole. The $c_6$ values were subsequently calculated.

For the five-body model developed by Klute and Berge [**44**], a total body mass of 90 kg was considered to calculate the model parameters. The mass of the prosthetic foot, pylon, and socket system $m_1$, the lower-body wobbling mass $m_2$, the lower-body rigid mass $m_3$, the upper-body wobbling mass $m_5$, and the upper-body rigid mass $m_4$ were estimated to be 2 per cent, 7 per cent, 6 per cent, 60 per cent, and 25 per cent of the total-body mass, respectively. The stiffness and damping coefficients of the rigid pylon, $k_2$ and $c_2$, were approximated from the material properties of a thin-walled aluminium tube. The stiffness and damping coefficients of the spring and the damper connecting the lower-body wobbling and rigid masses, $k_3$ and $c_3$, were estimated from the data provided by Cavagna [**51**]. Field observations of subjects walking and jumping were utilized to predict the vibration frequency of the upper-body wobbling mass and to subsequently estimate the upper-body stiffness constants $k_4$ and $k_5$. The upper-body damping coefficients $c_4$ and $c_5$ were approximated by applying the critical damping ratio assumption.

## 3 ACTIVE MODELS

There are two types of muscle activity during the bounce gait, namely pre-landing and post-landing muscle activities [**52**]. The pre-landing muscle activity is a preparatory mechanism of the human body to minimize impact shock or other undesirable effects of landing such as excessive joint rotation. The post-landing muscle activity is the active response of the human body to the forces experienced during the collision with the ground. In passive MSD models, the mechanical properties of the spring–damper elements of the model are considered to be constant regardless of the type of footwear, ground stiffness, etc. Neither pre-landing nor post-landing is therefore taken into account in passive MSD models. In active MSD models, the pre-landing activity of the lower-limb muscles is taken into account. The mechanical properties of the spring–damper elements are, therefore, no longer constant in an active model but are adjustable. A mechanism that mimics the functionality of the preparatory mechanism of the human body adjusts the properties of the lower-body soft tissues to minimize the undesirable effects that are defined in the model in terms of the cost function of an optimization process.

The GRF predicted with the passive MSD models is shown to be strongly dependent on the mechanical properties of the footwear [**26**, **39**]. This conclusion is in line with the observations in studies in which the leg is fixed and exposed to impact [**53**]. Nevertheless, experiments on actual runners showed no or little dependency of the GRF on the shoe type and/or stiffness of the running platform [**54**–**58**]. It has been suggested that the muscle activity during running is the reason why these two different types of experiments (fixed-leg and actual runners) yield different results [**59**].

There is a second experimental observation that concerns the level of vibrations during running. It is shown that the vibrations of soft tissues are heavily damped regardless of the parameters of the system (e.g. the stiffness of the footwear) [**60**]. Once more, it is proposed that muscle activity is responsible for this behaviour [**60**–**64**]. Similar to the GRF, it is shown that the level of vibrations predicted by a passive MSD model changes significantly when the properties of the footwear change [**65**].

Based on the above-mentioned experimental findings, an accurate MSD model should take the muscle activity into account. However, active models are not yet extensively developed. In a recent study, Zadpoor and Nikooyan [**66**] improved a previously developed model [**26**] in such a way that it can take the pre-landing muscle activity into account. A controller is added to the model shown in Fig. 5(a) and adjusts the stiffness and damping properties of the lower-body soft-tissue package ($k_2$ and $c_2$). Although the controller is meant to mimic the functionality of the central nervous system

(CNS) in adjusting the mechanical properties of the soft-tissue package, it is by no means similar to the CNS in terms of structure. The controller is a nonlinear optimizer that minimizes some objective functions that are based on two physiological hypotheses. The first objective function was designed based on the constant force hypothesis according to which the human body adjusts the mechanical properties of the lower-body soft tissues such that the changes in the GRF are minimal. The objective function, $J_f$, can be formulated as follows

$$J_f = |p_1\langle b_i, d_i\rangle - p_{1,0}\langle b_0, d_0\rangle| + |p_2\langle b_i, d_i\rangle - p_{2,0}\langle b_0, d_0\rangle| \quad (11)$$

where $p_1$ and $p_2$ are the first (impact) and second (active) peaks of the GRF (Fig. 2) as functions of the shoe hardness parameters, and $p_{1,0}$ and $p_{2,0}$ are the initial force peaks [**26**] calculated using the default shoe parameters $b_0$ and $d_0$ (Table 3).

The second objective function is based on the vibration hypothesis. According to this hypothesis, the human body adjusts the mechanical properties of the lower-body soft tissues such that the changes in the level of vibrations are minimal. The vibration level is quantified based on the amplitude $\Lambda$ of the displacements of the lower-body soft-tissue package. Based on the vibration hypothesis, the vibration amplitude cost function, $J_{v1}$, can be defined as

$$J_{v1} = |\Lambda_i\langle b_i, d_i\rangle - \Lambda_0\langle b_0, d_0\rangle| \quad (12)$$

The default values of the amplitude, $\Lambda_0$, are calculated using the default values of $b$ and $d$, i.e. $b_0$ and $d_0$. In a previous study of the authors [**65**], the values of $\Lambda_0$ were calculated. In addition to the cost function formulated by equation (12), another cost function was formulated using a different way of quantifying the vibration level. That second cost function is, however, not discussed here due to its failure in providing predictions that were in agreement with experimental observations [**66**].

The pattern search method was applied for bound-constrained minimization of the objective functions [**67**]. The independent variables of the objective function were the stiffness and damping coefficients $k_2$ and $c_2$ of the lower-body wobbling mass.

The simulation results using the force cost function $J_f$ showed that the improved model can predict the GRF that matches the experiments on actual runners. The model can also predict the vibration levels that are in agreement with the experimental observations when applying the vibration criterion $J_{v1}$. However, the predicted level of vibrations does not match experimental results when the constant force objective function is used. Similarly, the predicted GRF does not match experimental observations when the vibration objective function is employed. Thus, in a more recent study, Nikooyan and Zadpoor [**68**] introduced a combined cost function that matches experimental observations better. The improved cost function, $J_{fv}$, is the normalized sum of the two previously proposed (force and vibration) cost functions and is formulated as

$$J_{fv} = \left(\left|\frac{p_1\langle b_i, d_i\rangle - p_{1,0}}{p_{1,0}}\right| + \left|\frac{p_2\langle b_i, d_i\rangle - p_{2,0}}{p_{2,0}}\right|\right) + \left|\frac{\Lambda_i\langle b_i, d_i\rangle - \Lambda_0}{\Lambda_0}\right| \quad (13)$$

Nikooyan and Zadpoor [**68**] repeated their simulations using this improved cost function and showed that the new cost function can predict the GRF and vibration levels that are in agreement with experimental observations.

## 4 DISCUSSION

In this section, the pros and cons of the MSD models are discussed. First, the entire class of MSD models is compared with the class of musculoskeletal models. Even though these two classes of models are not parallel and differ in many aspects, they are sometimes compared [**2**] in the sense that both present mechanical models of locomotion. A comparison between these two classes of biomechanical models helps one put the MSD modelling approach in perspective. Second, a comparison is made between the different types of MSD models and the pros and cons of one-body versus multi-body models, and passive models versus active models, are discussed. Finally, possible future research trends in MSD modelling are presented.

### 4.1 Mass–spring–damper models versus musculoskeletal models

There are two major approaches to the modelling of the musculoskeletal system during locomotion, namely musculoskeletal (or detailed) modelling [**69**] and MSD (or simple) modelling. As mentioned already, these two approaches are quite different and are therefore not comparable in all aspects. However, they can be compared in a few aspects. For example, both modelling approaches try to describe locomotion using mechanical models. Moreover, both approaches provide some measures of the loading of the musculoskeletal system during locomotion.

Musculoskeletal modelling is based on detailed descriptions of the musculoskeletal system. The

detailed geometry of bones and their inertia properties, individual muscles and their lines of actions, and the accurate anatomical architecture of the musculoskeletal system are implemented in a sophisticated multi-body model. The models can be even scaled to account for the differences between different individuals (subject-specific musculoskeletal modelling [**70**]). These models can provide information about the state of individual muscles and body segments during locomotion. Moreover, they can be used for determining the detailed loading of skeletal tissues during locomotion. This type of information is useful, for example, in finite element modelling of skeletal tissues.

In MSD modelling approach, a limited number of lumped masses represent hard tissues and soft tissues. The number of elements present in a typical MSD model is generally far smaller than the number of elements present in a typical musculoskeletal system. Many tissues are lumped together and are represented as one single element of the model. Due to the limited number of elements present in the MSD models, they are far easier to understand and simulate. Therefore, it is much easier to determine the parameters of an MSD system. Moreover, one can more easily implement the lesser-known aspects of locomotion in MSD models. This is because the overall complexity of the system including the additional complexity caused by the aspect under study is less. Moreover, one does not need many parameters for implementation of the lesser-known aspects of locomotion in an MSD model. The governing equations of motion are also much easier to derive and to solve numerically. The simplicity of MSD models comes at the cost of accuracy. Moreover, the loading of the skeletal system that is predicted by MSD models is not detailed enough to be used, for example, in finite element modelling of skeletal tissues. One of the consequences of the simplicity of MSD models is that they can be more easily used for pedagogical purposes such as teaching the biomechanical modelling of locomotion. Furthermore, MSD models are used in the design and analysis of other moving objects such as humanoid legged robots [**71**, **72**].

### 4.2 One-body versus multi-body models

The one-body models are simple and need few parameters. Due to their simplicity, it is easier to connect experimental observations and model predictions. As explained in previous sections, the stiffness of the human body during running is often calculated using the one-body models. However, one-body models are not capable of producing the actual pattern of the GRF. In particular, the GRF resulting from simulation of one-body models is always with one peak (Fig. 2). It is well known that the GRF has two distinct peaks (Fig. 2) in many cases. Multi-body models are more complicated and need more parameters, meaning that the determination of the parameters of multi-body systems is not as easy as for one-body systems. Connecting experimental observations to simulation results is also more difficult. There is no such a thing as the stiffness of the human body when multi-body systems are used. There are several stiffness values and a parameter identification procedure is normally needed for matching the experimental observations with simulation results. However, multi-body models are more capable than one-body systems and can produce the actual shape of the GRF including two distinct peaks. In addition, several phenomena that cannot be studied using the one-body can be studied using a multi-body system. For example, one could study the isolated effects of the wobbling mass on the dynamic behaviour of the human body during running.

### 4.3 Active versus passive models

Passive models do not take the muscle activity into account. The muscle activity during running is known to be associated with changes in the stiffness of soft tissues [**26**]. Neglecting the muscle activity means that the validity of the simulation results of the passive models is limited to the cases where there is not much change in the stiffness of soft tissues. Active models take the muscle activity into account and are therefore capable of coping with the changes in the stiffness of soft tissues. However, the development of the active models has just recently started and the currently available active models are capable only of taking the pre-landing muscle activity into account. The post-landing muscle activity needs to be also taken into account in order to enhance the range of the validity of active models.

### 4.4 Future research trends

There are several aspects of MSD models that need further improvement. One of the limitations associated with most multi-body models is that they can only capture the vertical behaviour of the body during locomotion. A natural enhancement of multi-body MSD models is to incorporate the effects of contact angle (similar to the 2D motion one-body model presented in section 2.1). The other limitations of MSD models are the lack of a standard

procedure for determination of their parameters and the lack of appropriately determined parameters. Since a lot of effort has been put into accurate determination of the parameters of musculoskeletal systems, the authors propose that one can use musculoskeletal systems to determine the parameters of MSD models. A standard computational procedure is needed for that purpose.

Active models are a relatively new subcategory of MSD models. Several enhancements are needed in order to make this subcategory of models capable of accurately simulating the interplay between the neural system and musculoskeletal system during running. For example, the post-landing muscle activities need to be implemented in the models. The merit of the proposed cost functions needs to be researched as well to determine whether or not they provide predictions that are in agreement with detailed experimental observations. Depending on the results of the validation study, additional cost functions may be needed. These enhancements will improve the usability of MSD models particularly in the areas where they were not previously used.

## 5 CONCLUSIONS

The MSD models developed for simulation of the mechanics of the human body during running and hopping were reviewed in the present paper. The different categories of these models were covered including active and passive one-body and multi-body models. The governing equations of motion of the models as well as their parameters were presented. The pros and cons of the different types of MSD models were discussed. It was shown that even though these models are not detailed enough to be used for prediction of the detailed loading of skeletal tissues during bouncing gait, they can be used in a descriptive capacity for studying the general principles of running and hopping.

## FUNDING

This research received no specific grant from any funding agency in the public, commercial, or not for profit sectors.



## REFERENCES

1 **Liu, W.** and **Nigg, B. M.** A mechanical model to determine the influence of masses and mass distribution on the impact force during running. *J. Biomech.*, 2000, **33**(2), 219–224.
2 **Bullimore, S. R.** and **Burn, J. F.** Ability of the planar spring–mass model to predict mechanical parameters in running humans. *J. Theor. Biol.*, 2007, **248**(4), 686–695.
3 **Blickhan, R.** The spring–mass model for running and hopping. *J. Biomech.*, 1989, **22**(11–12), 1217–1227.
4 **McMahon, T. A.** and **Cheng, G. C.** The mechanics of running: how does stiffness couple with speed? *J. Biomech.*, 1990, **23**(Suppl. 1), 65–78.
5 **Farley, C. T.** and **González, O.** Leg stiffness and stride frequency in human running. *J. Biomech.*, 1996, **29**(2), 181–186.
6 **Dalleau, G., Belli, A., Bourdin, M.,** and **Lacour, J. R.** The spring–mass model and the energy cost of treadmill running. *Eur. J. Appl. Physiol.*, 1998, **77**(3), 257–263.
7 **Heise, G. D.** and **Martin, P. E.** 'Leg spring' characteristics and the aerobic demand of running. *Med. Sci. Sports Exerc.*, 1998, **30**(5), 750–754.
8 **Farley, C. T., Glasheen, J.,** and **McMahon, T. A.** Running springs: speed and animal size. *J. Exp. Biol.*, 1993, **185**(1), 71–86.
9 **Arampatzis, A., Brüggemann, G.-P.,** and **Metzler, V.** The effect of speed on leg stiffness and joint kinetics in human running. *J. Biomech.*, 1999, **32**(12), 1349–1353.
10 **Ferris, D. P., Louie, M.,** and **Farley, C. T.** Running in the real world: adjusting leg stiffness for different surfaces. *Proc. R. Soc. B, Biol. Sci.*, 1998, **265**(1400), 989–994.
11 **Kerdok, A. E., Biewener, A. A., McMahon, T. A., Weyand, P. G.,** and **Herr, H. M.** Energetics and mechanics of human running on surfaces of different stiffnesses. *J. Appl. Physiol.*, 2002, **92**(2), 469–478.
12 **Dutto, D. J.** and **Smith, G. A.** Changes in spring–mass characteristics during treadmill running to exhaustion. *Med. Sci. Sports Exerc.*, 2002, **34**(8), 1324–1331.
13 **Donelan, J. M.** and **Kram, R.** Exploring dynamic similarity in human running using simulated reduced gravity. *J. Exp. Biol.*, 2000, **203**(16), 2405–2415.
14 **He, J. P., Kram, R.,** and **McMahon, T. A.** Mechanics of running under simulated low gravity. *J. Appl. Physiol.*, 1991, **71**(3), 863–870.
15 **Seyfarth, A., Geyer, H., Gunther, M.,** and **Blickhan, R.** A movement criterion for running. *J. Biomech.*, 2002, **35**(5), 649–655.
16 **Farley, C. T., Blickhan, R., Saito, J.,** and **Taylor, C. R.** Hopping frequency in humans: a test of how springs set stride frequency in bouncing gaits. *J. Appl. Physiol.*, 1991, **71**(6), 2127–2132.
17 **Hobara, H., Inoue, K., Gomi, K., Sakamoto, M., Muraoka, T., Iso, S.,** and **Kanosue, K.** Continuous change in spring–mass characteristics during a 400 m sprint. *J. Sci. Med. Sport*, 2009, **13**(2), 256–261.
18 **Butler, R. J., Crowell, H. P.,** and **Davis, I. M.** Lower extremity stiffness: implications for performance and injury. *Clin. Biomech.*, 2003, **18**(6), 511–517.

19 **Blum, Y., Lipfert, S. W.,** and **Seyfarth, A.** Effective leg stiffness in running. *J. Biomech.*, 2009, **42**(14), 2400–2405.

20 **Hunter, I.** A new approach to modeling vertical stiffness in heel–toe distance runners. *J. Sports Sci. Med.*, 2003, **2**, 139–143.

21 **Bullimore, S. R.** and **Burn, J. F.** Consequences of forward translation of the point of force application for the mechanics of running. *J. Theor. Biol.*, 2006, **238**(1), 211–219.

22 **Cavagna, G. A.** Force platforms as ergometers. *J. Appl. Physiol.*, 1975, **39**(1), 174–179.

23 **Cavagna, G. A., Franzetti, P., Heglund, N. C.,** and **Willems, P.** The determinants of the step frequency in running, trotting and hopping in man and other vertebrates. *J. Physiol.*, 1988, **399**, 81–92.

24 **McMahon, T. A., Valiant, G.,** and **Frederick, E. C.** Groucho running. *J. Appl. Physiol.*, 1987, **62**(6), 2326–2337.

25 **Zadpoor, A. A.** and **Nikooyan, A. A.** The relationship between lower-extremity stress fractures and the ground reaction force: a systematic review. *Clin. Biomech.*, 2010, **26**(1), 23–28.

26 **Zadpoor, A. A., Nikooyan, A. A.,** and **Arshi, A. R.** A model-based parametric study of impact force during running. *J. Biomech.*, 2007, **40**(9), 2012–2021.

27 **Bennell, K., Crossley, K., Jayarajan, J., Walton, E., Warden, S., Kiss, Z. S.,** and **Wrigley, T.** Ground reaction forces and bone parameters in females with tibial stress fracture. *Med. Sci. Sports Exerc.*, 2004, **36**(3), 397–404.

28 **Creaby, M. W.** and **Dixon, S. J.** External frontal plane loads may be associated with tibial stress fracture. *Med. Sci. Sports Exerc.*, 2008, **40**(9), 1669–1674.

29 **Crossley, K., Bennell, K. L., Wrigley, T.,** and **Oakes, B. W.** Ground reaction forces, bone characteristics, and tibial stress fracture in male runners. *Med. Sci. Sports Exerc.*, 1999, **31**(8), 1088–1093.

30 **Dixon, S. J., Creaby, M. W.,** and **Allsopp, A. J.** Comparison of static and dynamic biomechanical measures in military recruits with and without a history of third metatarsal stress fracture. *Clin. Biomech.*, 2006, **21**(4), 412–419.

31 **Divert, C., Mornieux, G., Baur, H., Mayer, F.,** and **Belli, A.** Mechanical comparison of barefoot and shod running. *Int. J. Sports Med.*, 2005, **26**(7), 593–598.

32 **Grimston, S. K., Engsberg, J. R., Kloiber, R., Loiber, R.,** and **Hanley, D. A.** Bone mass, external loads, and stress fractures in female runners. *J. Appl. Biomech.*, 1991, **7**(3), 293–302.

33 **Wheat, J. S., Bartlett, R. M., Milner, C. E.,** and **Mullineaux, D. R.** The effect of different surfaces on ground reaction forces during running: a single-individual design approach. *J. Hum. Mov. Stud.*, 2003, **44**(5), 353–364.

34 **Alexander, R. M., Bennett, M. B.,** and **Ker, R. F.** Mechanical properties and function of the paw pads of some mammals. *J. Zool.*, 1986, **209**(3), 405–419.

35 **Mizrahi, J.** and **Susak, Z.** *In-vivo* elastic and damping response of the human leg to impact forces. *J. Biomech. Engng, Trans. ASME*, 1982, **104**(1), 63–66.

36 **Nevzat Özgüven, H.** and **Berme, N.** An experimental and analytical study of impact forces during human jumping. *J. Biomech.*, 1988, **21**(12), 1061–1066.

37 **Derrick, T. R., Caldwell, G. E.,** and **Hamill, J.** Modeling the stiffness characteristics of the human body while running with various stride lengths. *J. Appl. Biomech.*, 2000, **16**(1), 36–51.

38 **Kim, W., Voloshin, A. S.,** and **Johnson, S. H.** Modeling of heel strike transients during running. *Hum. Mov. Sci.*, 1994, **13**(2), 221–244.

39 **Nigg, B. M.** and **Liu, W.** The effect of muscle stiffness and damping on simulated impact force peaks during running. *J. Biomech.*, 1999, **32**(8), 849–856.

40 **Yue, Z.** and **Mester, J.** A model analysis of internal loads, energetics, and effects of wobbling mass during the whole-body vibration. *J. Biomech.*, 2002, **35**(5), 639–647.

41 **Yue, Z.** and **Mester, J.** A modal analysis of resonance during the whole-body vibration. *Stud. Appl. Math.*, 2004, **112**(3), 293–314.

42 **Zadpoor, A. A.** and **Nikooyan, A. A.** A mechanical model to determine the influence of masses and mass distribution on the impact force during running – a discussion. *J. Biomech.*, 2006, **39**(2), 388–390.

43 **Ly, Q. H., Alaoui, A., Erlicher, S.,** and **Baly, L.** Towards a footwear design tool: influence of shoe midsole properties and ground stiffness on the impact force during running. *J. Biomech.*, 2010, **43**(2), 310–317.

44 **Klute, G.** and **Berge, J.** Modelling the effect of prosthetic feet and shoes on the heel–ground contact force in amputee gait. *Proc. IMechE, Part H: J. Engineering in Medicine*, 2004, **218**(3), 173–182.

45 **Williams, M.** and **Lessner, H.** *Biomechanics of human motion*, 1966 (Saunders, Philadelphia, Pennsylvania).

46 **Cole, G. K.** Loading of the joints of the lower extremities during the impact phase in running, Ph.D. dissertation, Department of Mechanical Engineering, The University of Calgary, Calgary, Canada, 1995.

47 **Clarys, J. P.** and **Marfell-Jones, M. J.** Anthropometric prediction of component tissue masses in the minor limb segments of the human body. *Hum. Biol.*, 1986, **58**(5), 761–769.

48 **Clauser, C. E., McConville, J. T.,** and **Young, J. W.** Weight, volume, and center of mass of segments of the human body, Wright-Patterson Air Force Base, Dayton, Ohio, 1969.

49 **Hoerler, E.** Mechanisches Modell zur Beschreibung des isometrischen und des dynamischen Muskelkraftverlaufs. *Jugend und Sport*, 1972, **29**, 271–273.

50 **Aerts, P.** and **De Clercq, D.** Deformation characteristics of the heel region of the shod foot during a simulated heel strike: the effect of varying midsole hardness. *J. Sports Sci.*, 1993, **11**(5), 449–461.

51 **Cavagna, G. A.** Elastic bounce of the body. *J. Appl. Physiol.*, 1970, **29**(3), 279–282.

52 **Santello, M.** Review of motor control mechanisms underlying impact absorption from falls. *Gait Posture*, 2005, **21**(1), 85–94.

53 **Lafortune, M. A., Hennig, E. M.,** and **Lake, M. J.** Dominant role of interface over knee angle for cushioning impact loading and regulating initial leg stiffness. *J. Biomech.*, 1996, **29**(12), 1523–1529.

54 **Bates, B. T., Osternig, L. R., Sawhill, J. A.,** and **James, S. L.** An assessment of subject variability, subject–shoe interaction, and the evaluation of running shoes using ground reaction force data. *J. Biomech.*, 1983, **16**(3), 181–191.

55 **Clarke, T. E., Frederick, E. C.,** and **Cooper, L. B.** The effects of shoe cushioning upon ground reaction forces in running. *Int. J. Sports Med.*, 1983, **4**(4), 247–251.

56 **De Wit, B., De Clercq, D.,** and **Aerts, P.** Biomechanical analysis of the stance phase during barefoot and shod running. *J. Biomech.*, 2000, **33**(3), 269–278.

57 **Dixon, S. J., Collop, A. C.,** and **Batt, M. E.** Surface effects on ground reaction forces and lower extremity kinematics in running. *Med. Sci. Sports Exerc.*, 2000, **32**(11), 1919–1926.

58 **Lieberman, D. E., Venkadesan, M., Werbel, W. A., Daoud, A. I., D'Andrea, S., Davis, I. S., Mang'Eni, R. O.,** and **Pitsiladis, Y.** Foot strike patterns and collision forces in habitually barefoot versus shod runners. *Nature*, 2010, **463**(7280), 531–535.

59 **Nigg, B. M., Stefanyshyn, D., Cole, G., Stergiou, P.,** and **Miller, J.** The effect of material characteristics of shoe soles on muscle activation and energy aspects during running. *J. Biomech.*, 2003, **36**(4), 569–575.

60 **Wakeling, J. M., Liphardt, A. M.,** and **Nigg, B. M.** Muscle activity reduces soft-tissue resonance at heel-strike during walking. *J. Biomech.*, 2003, **36**(12), 1761–1769.

61 **Wakeling, J. M.** and **Nigg, B. M.** Modification of soft tissue vibrations in the leg by muscular activity. *J. Appl. Physiol.*, 2001, **90**(2), 412–420.

62 **Wakeling, J. M., Nigg, B. M.,** and **Rozitis, A. I.** Muscle activity in the lower extremity damps the soft-tissue vibrations which occur in response to pulsed and continuous vibrations. *J. Appl. Physiol.*, 2002, **93**(3), 1093–1103.

63 **Wakeling, J. M., Pascual, S. A.,** and **Nigg, B. M.** Altering muscle activity in the lower extremities by running with different shoes. *Med. Sci. Sports Exerc.*, 2002, **34**(9), 1529–1532.

64 **Wakeling, J. M., Von Tscharner, V., Nigg, B. M.,** and **Stergiou, P.** Muscle activity in the leg is tuned in response to ground reaction forces. *J. Appl. Physiol.*, 2001, **91**(3), 1307–1317.

65 **Nikooyan, A. A.** and **Zadpoor, A. A.** A model-based parametric study of soft tissue vibrations during running. In Proceedings of the Annual Symposium of the *IEEE-EMBS Benelux Chapter*, Heeze, The Netherlands, 6–7 December 2007, pp. 49–52 (IEEE).

66 **Zadpoor, A. A.** and **Nikooyan, A. A.** Modeling muscle activity to study the effects of footwear on the impact forces and vibrations of the human body during running. *J. Biomech.*, 2010, **43**(2), 186–193.

67 **Lewis, R.** and **Torczon, V.** Pattern search algorithms for bound constrained minimization. *SIAM J. Optim.*, 1999, **9**(4), 1082–1099.

68 **Nikooyan, A. A.** and **Zadpoor, A. A.** An improved cost function for modeling of muscle activity during running. *J. Biomech.*, 2011, **44**(5), 984–987.

69 **Nikooyan, A. A., Veeger, H. E. J., Westerhoff, P., Graichen, F., Bergmann, G.,** and **van der Helm, F. C. T.** Validation of the Delft Shoulder and Elbow Model using *in-vivo* glenohumeral joint contact forces. *J. Biomech.*, 2010, **43**(15), 3007–3014.

70 **Scheys, L., Jonkers, I., Schutyser, F., Pans, S., Spaepen, A.,** and **Suetens, P.** Image based methods to generate subject-specific musculoskeletal models for gait analysis. *International Congress Series*, 2005, **1281**, 62–67.

71 **Kawamura, A.** and **Chi, Z.** One-leg jumping with virtual spring principle. In Proceedings of the 8th IEEE-RAS International Conference on *Humanoid Robots*, Daejeon, Korea, 1–3 December 2008, Article number 4755928, pp. 34–39 (IEEE). DOI: 10.1109/ICHR.2008.4755928

72 **Tamaddoni, S. H., Alasty, A., Meghdari, A., Sohrabpour, S.,** and **Salarieh, H.** Spring–mass jumping of underactuated biped robots. In Proceedings of ASME *International Design Engineering Technical Conferences and Computers and Information in Engineering Conference*, Las Vegas, Nevada, 2007, vol. 5, part C, pp. 1923–1930 (ASME, New York, USA).